Russian Journal of Nonlinear Dynamics, 2019, vol. 15, no. 4, pp. 561–568.
Full-texts are available at http://nd.ics.org.ru
DOI: 10.20537/nd190415

MSC 2010: 93C10, 93C15

Sub-Riemannian Geometry in Image Processing and Modeling of the Human Visual System

A. P. Mashtakov

This paper summarizes results of a sequence of works related to usage of sub-Riemannian (SR) geometry in image processing and modeling of the human visual system. In recent research in psychology of vision (J. Petitot, G. Citti, A. Sarti) it was shown that SR geodesics appear as natural curves that model a mechanism of the primary visual cortex V1 of a human brain for completion of contours that are partially corrupted or hidden from observation. We extend the model to include data adaptivity via a suitable external cost in the SR metric. We show that data adaptive SR geodesics are useful in real image analysis applications and provide a refined model of V1 that takes into account the presence of a visual stimulus.

Keywords: sub-Riemannian, detection of salient lines, vision, visual cortex, brain-inspired methods

1. Introduction

This paper is devoted to usage of sub-Riemannian (SR) geometry in image processing and modeling of the human visual system. It summarizes the results of joint works [1–5]. In recent research in psychology of vision [6, 7] it was shown that SR geodesics appear as natural curves that model a mechanism of the primary visual cortex V1 of a human brain for completion of contours that are partially corrupted or hidden from observation, see Fig. 1.

Received May 31, 2019
Accepted September 03, 2019

This work was supported by the Russian Science Foundation under grant 17-11-01387 and performed at the Ailamazyan Program Systems Institute of the Russian Academy of Sciences.

Alexey P. Mashtakov
alexey.mashtakov@gmail.com
Ailamazyan Program Systems Institute of RAS
Pereslavl-Zalessky, Yaroslavl Region, 152020 Russia

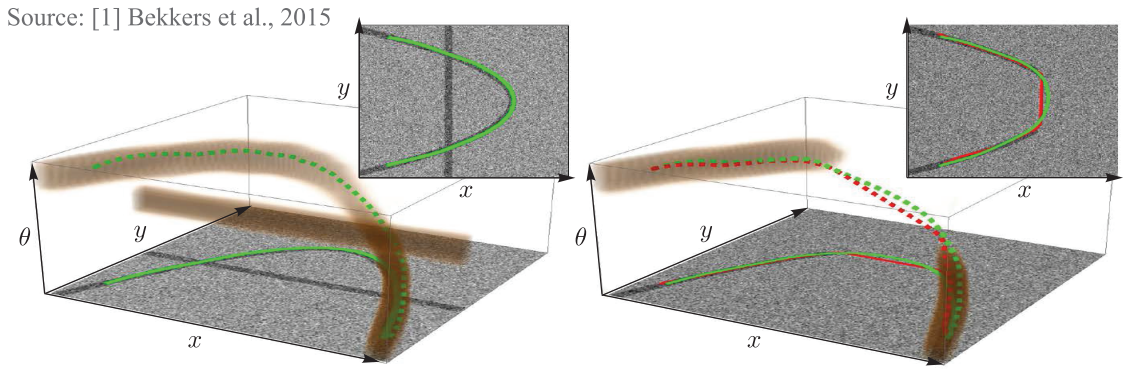

Fig. 1. In order to process the visual signal, the primary visual cortex V1 lifts the image from the retinal plane $(x, y) \in \mathbb{R}^2$ to the extended space of positions and orientations $(x, y, \theta) \in \mathbb{R}^2 \times S^1$, where crossing structures are disentangled. If part of the contour is hidden from observation, the gap is restored via a SR geodesic, which follows the curvilinear structure along the gap better than a Riemannian geodesic.

Understanding of mechanisms of vision of mammals has been an attracting topic for many researchers in recent years. The investigation of Hubel and Wiesel (Nobel Prize in Physiology or Medicine, 1981) has produced a strong progress in understanding of the functional architecture of the primary visual cortex V1. Hubel and Wiesel have realized that specific neurons in the visual areas of the cerebral cortex are connected to certain areas of the visual field of the retina. They performed an experiment showing that the neurons in different areas of the visual cortex react to various orientations at the same position in the visual field. It was understood that, for efficient image processing, the brain stores the image not as a sequence of points, but as a sequence of strokes (points and directions tangential to the contour). Thus, a contact structure in the extended space of positions and orientations over the retina naturally appears in the modeling of V1.

Therefore, Petitot [6], Citti and Sarti [7] suggested modeling V1 by a SR contact structure on Lie groups H_3 and SE_2. In their model, the retina is represented by a real plane, and SR geodesics arise naturally as the curves that minimize the energy expended to create a connection between the excited neurons.

The paper has the following structure. In Section 2, we explain the basic concepts of SR geometry and present a method to compute SR minimizers for 2-bracket generating SR structures on 3D and 6D Lie groups. Then, in Section 3, we show how they provide brain inspired methods in computer vision. We discuss how considering SR structures on 2D and 3D images (or more precisely, on their lift to the extended space of positions and directions) helps to detect some features, e.g., salient curves in images. We consider several particular examples: tracking of blood vessels in planar and spherical images of human retina, and tracking of neural fibers in MRI images of the human brain. Afterwards, in Section 4 we show how a proper choice of the external cost in SR metric based on a response of simple cells to the visual stimulus provides a model for geometrical optical illusions.

2. A brief tour of SR geometry on Lie Groups

Sub-Riemannian geometry is a rapidly developing domain of mathematics at the crossroads of differential geometry, PDEs, optimal control and calculus of variations, metric analysis, Lie groups and Lie algebras theory, and other important domains, with rich applications to mechanics, robotics, neurophysiology and vision, etc [9].

Let G be a connected n-dimensional Lie group with unit element e, and L the Lie algebra of left-invariant vector fields on G. A *SR structure* on G is a left-invariant subbundle $\Delta \subset TG$, $\dim \Delta|_g = d$ for all $g \in G$, endowed with an inner product $\mathcal{G}$ in Δ. In this paper, we choose $d = 2, 3$ and consider a 2-bracket generating SR structures $\Delta + [\Delta, \Delta] = TG$. In such a way, we consider $n = 3, 6$-dimensional Lie groups G.

A Lipschitzian curve $\gamma : [0, T] \to G$ is called *horizontal* if $\dot\gamma(t) \in \Delta_{\gamma(t)}$ for a.e. $t \in [0, T]$.

A *SR minimizer* is a horizontal curve that has a minimum length

$$l(\gamma) = \int_0^T \sqrt{\mathcal{G}(\dot\gamma(t), \dot\gamma(t))}\, dt \to \min$$

among all horizontal curves connecting the same end points.

A SR structure can be defined by an orthonormal frame $X_1, \dots, X_d \in L$:

$$\Delta = \operatorname{span}(X_1, \dots, X_d), \quad \mathcal{G}(X_i, X_j) = \delta_{ij}, \quad i, j = 1, \dots, d. \tag{2.1}$$

Then a SR minimizer connecting e and g is a solution to the optimal control problem

$$\dot\gamma = \sum_{i=1}^{d} u_i X_i, \quad \gamma(0) = e,\ \gamma(T) = g, \quad l(\gamma) = \int_0^T \sqrt{u_1^2 + \ldots + u_d^2}\, dt \to \min, \tag{2.2}$$

where $g \in G$ and $u_i(\cdot)$ are real-valued L^∞ functions, which are called the controls.

By the Rashevskii – Chow and Filippov theorems, there always exists a SR minimizer connecting e and g. Thus, one has a well-defined *SR distance* map

$$d(e, g) = \min \left\{ l(\gamma) \;\middle|\; \gamma \in \operatorname{Lip}([0, T], G),\ \gamma(0) = e, \gamma(T) = g,\ \dot\gamma(t) \in \Delta_{\gamma(t)} \right\}.$$

A *SR geodesic* is a curve in G whose sufficiently short arcs are SR minimizers. A classical approach to computing SR geodesics is based on Pontryagin's maximum principle (PMP) [10, 11]. Application of PMP to the problem (2.2) leads to the Hamiltonian system $\dot\lambda = \vec H(\lambda)$ that describes any geodesic via the initial value $\lambda_0 = \lambda(0)$. Here, $\lambda \in T^*G$ is the momentum covector, and $\vec H(\lambda)$ is the Hamiltonian vector field with the Hamiltonian $H(\lambda)$. Parametrization of the geodesics by arclength implies $H(\lambda) = \frac{1}{2}$.

Thus, according to the classical approach, SR geodesics are found as solutions to the Hamiltonian system of PMP. The next step is to select SR minimizers among SR geodesics via second-order optimality conditions, which is the most difficult step. It is known (see, e.g., [9, 10]) that sufficiently short arcs of SR geodesics are SR minimizers (optimal trajectories). It is also known that in general a geodesic loses its optimality after a *cut point*. The corresponding instance of time is called *cut time*, and the set of all cut points forms the so-called *cut locus*. Note that the structure of cut locus for the SR structures on Lie groups is known only in some special cases [12].

A useful tool for studying SR geodesics on a Lie group G is *the exponential map*[1], which maps an initial momentum λ_0 and a time t to the end point of the corresponding geodesic γ (i.e., the exponential map integrates the Hamiltonian system of PMP):

$$\exp : T_e^*G \times \mathbb{R} \to G,\ (\lambda_0, t) \mapsto \gamma(t). \tag{2.3}$$

[1]Not to be confused with the exponential map from Lie algebra to Lie group.

The wavefront consists of end points of all the geodesics of the same length T:

$$\mathrm{WF}(T) = \left\{ \exp(\lambda_0, T) \;\middle|\; \lambda_0 \in T^*_e G,\ H(\lambda_0) = \frac{1}{2} \right\}. \tag{2.4}$$

The outer surface of the wavefront forms a *sub-Riemannian sphere*, which is a set of endpoints in G equidistant from e:

$$\mathrm{S}(T) = \left\{ \exp(\lambda_0, T) \;\middle|\; \lambda_0 \in T^*_e G, H(\lambda_0) = \frac{1}{2}, t_{cut}(\lambda_0) \geqslant T \right\} = \left\{ g \in G \;\middle|\; d(e,g) = T \right\},$$

where $t_{cut}(\lambda_0)$ denotes the cut time for the geodesic with the initial momentum λ_0.

The classical approach for computation of SR minimizers via the Hamiltonian formalism is a powerful method that gives an exact expression for the SR distance and SR minimizers. Note that, due to the absence of knowledge about cut locus, the classical approach is applicable only in some special simplest cases. On the other hand, in applications, numerical solution is usually enough. Another approach, which we call the PDE approach, has been presented in [1]. It leads to an efficient numerical scheme to compute SR minimizers and consists in the following steps:

- Derivation of the Hamilton – Jacobi – Bellman (HJB) system, which describes propagation of the wavefront $\mathrm{WF}(t)$ for $t \in [0, T]$;
- Computation of the SR distance map as a viscosity solution of the HJB system;
- Finding the SR minimizers by the steepest descent on the distance function.

The advantage of the PDE approach is that it allows extension to non-uniform external cost $\mathcal{C}$ in SR metric

$$\mathcal{G}|_g = \mathcal{C}^2(g) \sum_{i=1}^{d} \omega^i|_g \otimes \omega^i|_g, \text{ for all } g \in G,$$

where $\omega^i \in T^*G$ are basis left-invariant one-forms, dual to X_i: $\langle \omega^i, X_j \rangle = \delta_{ij}$.

Expressing the HJB system in eikonal form leads to the following theorem:

Theorem 1. *Let $\mathcal{W}(g)$ be a viscosity solution of the eikonal system*

$$\begin{cases} \sum\limits_{i=1}^{d} (X_i|_g(\mathcal{W}))^2 = \mathcal{C}^2(g), \ \textit{for } g \neq e, \\ \mathcal{W}(e) = 0. \end{cases}$$

Then

- *$\mathcal{W}(g) = d(e,g)$ is the SR distance map;*
- *$\mathcal{S}_t = \{g \in G \mid \mathcal{W}(g) = t\}$ are SR-spheres $\mathrm{S}(t)$ of radius t;*
- *SR-minimizer $\gamma(t)$ connecting e to g is given by $\gamma(t) = \gamma_b(\mathcal{W}(g) - t)$, where $\gamma_b(t)$ is found by integration for $t \in [0, \mathcal{W}(g)]$*

$$\dot{\gamma}_b(t) = -\,u_1(t) X_1|_{\gamma_b(t)} - \ldots - u_d(t)\, X_d|_{\gamma_b(t)}\,, \qquad \gamma_b(0) = g,$$

where $u_i(t) = \dfrac{X_i|_{\gamma_b(t)}(\mathcal{W})}{\mathcal{C}^2(\gamma_b(t))}$, $i = 1, \ldots, d$.

2.1. Riemannian approximation and fast marching

One of the most efficient methods to compute geodesics in the Euclidean setting is fast marching, introduced by Sethian in [13]. It has been extended to the case of highly anisotropic Riemannian metric by Mirebeau [14]. Later on, this method was adapted for computation of SR minimizers (or more precisely, their Riemannian approximation) by Sanguinetti et al. in [15].

The usage of fast marching for computation of SR minimizers relies on Riemannian approximation of SR structure on G. In [16] convergence of the Riemannian distance to the SR distance was shown via the limiting procedure for the Riemannian metric

$$\mathcal{G}^{\varepsilon}|_g = \mathcal{C}^2(g)\left(\sum_{i=1}^{d}\omega^i|_g \otimes \omega^i|_g + \frac{1}{\varepsilon^2}\sum_{j=d+1}^{n}\omega^j|_g \otimes \omega^j|_g\right), \text{ for all } g \in G,$$

as $\varepsilon \to 0$.

3. Detection of salient curves in images

In this section, we show that data adaptive SR minimizers are useful in real image analysis applications and help to detect some features, e.g., salient curves in images. In computer vision, it is common to extract salient curves in images via data-driven minimal paths or geodesics [18]. The minimizing geodesic is defined as the curve that minimizes the length functional, which is typically weighted by a cost function with high values at image locations with low curve saliency. As an illustration, see Fig. 2, where we consider medical image analysis application — automatic extraction of the vascular retinal tree on images. It is helpful for early detection of many diseases, such as diabetic retinopathy, glaucoma, atherosclerosis, etc. (see, e.g., [17]).

Another set of geodesic methods, inspired by the psychology of vision, was developed in [6, 7]. The combination of such contour perception models with data adaptive geodesic methods has been presented in [1]. There, a computational framework for tracking of salient curves via globally optimal data adaptive sub-Riemannian geodesics on the Euclidean motion group SE_2 has been presented. In [1] the framework was used for tracking of retinal vessels in flat images of retina, see Fig. 3, left.

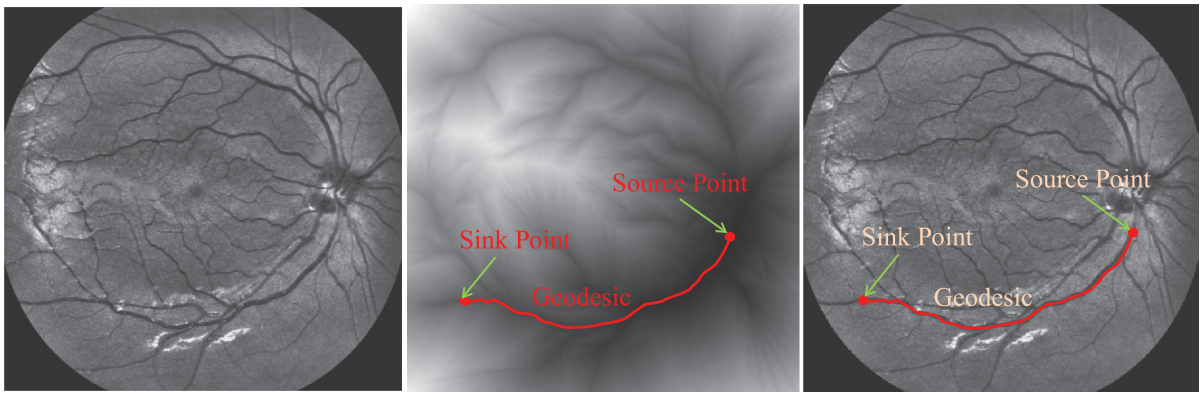

Image of Human Retina | Distance from Source Point | Vessel Tracking via Geodesic

Fig. 2. Geodesic methods are used for detection of salient lines on images, e.g., detection of vessels in images of human retina. They are based on computation of the distance map from a source point and on the consequent steepest descent on the distance map from a sink point. The resulting data adaptive geodesic accurately follows the vessel location.

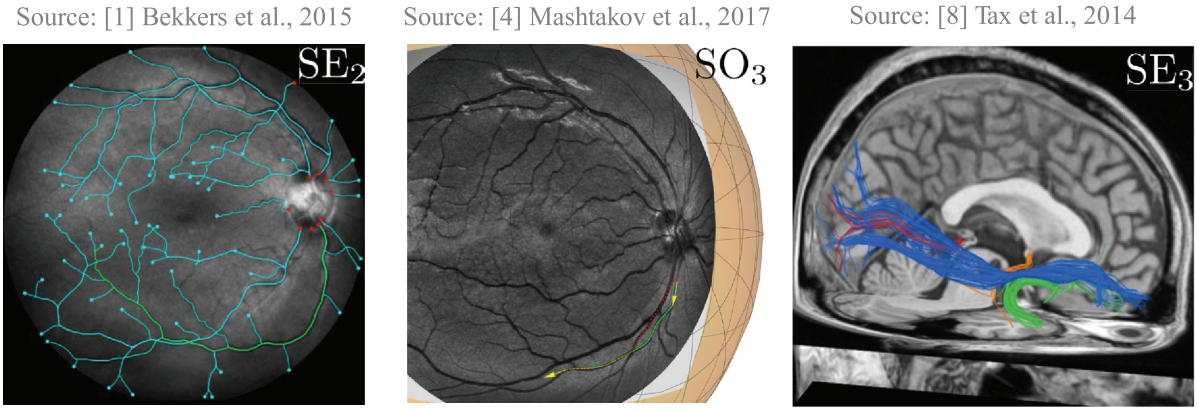

Fig. 3. Data adaptive SR minimizers in real image analysis applications: in Lie groups SE_2 and SO_3 they are used for tracking of blood vessels in flat and spherical images of human retina; in SE_3 they are used for tracking of neural fibers in MRI images of a human brain.

In [4] we show that optical retinal images are mostly acquired by flat cameras and, as a result, distortion appears. Such distortion could lead to questionable (distorted) geometrical features (vessel curvature, thickness, etc.) that are used as biomarkers for different diseases. We show that the distortion that appears near the boundary of a flat image can play a significant role in the quantitative analysis of the vascular structure and its curvature. In this work we extend the framework [1] for tracking of vessels in spherical images of the retina with reduced distortion. This requires a SR structure in the group SO_3 acting transitively on the 2-sphere S^2. See Fig. 3, middle.

Finally, we note that, in the same way as for 2D images, extraction of salient curves in 3D images results in tracking via SR geodesics in SE_3, see Fig. 3, right. In [2, 3] we study the SR problem in SE_3. In particular, we derive an explicit expression for extremal controls in a special case, which appears in applications, and derive the explicit formulas for SR geodesics before the first cusp point in their spatial projection.

4. Modeling of geometrical optical illusions

Geometrical-optical illusions (GOIs) have been discovered in the 19th century. They are defined as situations in which there is an awareness of a mismatch of geometrical properties between an item in the object space and its associated perception. These illusions induce a misjudgment of the geometrical properties of the visual stimulus, due to the perceptual difference between the features of the presented stimulus and its associated perceptual representation.

In [5], we propose a mathematical model for GOIs based on the functional architecture of V1. This neuro-mathematical model allows one to interpret at a neural level the origin of GOIs. The main idea is to adapt the model [7] for the functional geometry of V1 for perceptual completion. We extend the model to include data adaptivity via a suitable external cost in the SR metric. We show that data adaptive SR geodesics provide a refined model of V1 that takes into account the presence of a visual stimulus. We also postulate that illusory contours arise as geodesics in this new connectivity metric between two given sets. It requires adapting the fast marching algorithm, initially introduced as a tool for computing geodesics with fixed two-point boundary conditions.

We develop the idea that the SR metric is modulated by the output of the simple cells in V1, induced by the presence of a visual stimulus: cells already activated by the output are more sensitive to cortical propagation. In this way we define the external cost $\mathcal{C}(g)$ in accordance with the output of simple cells modeled by Gabor filters.

See Fig. 4 for the result of modeling for the round Poggendorff illusion.

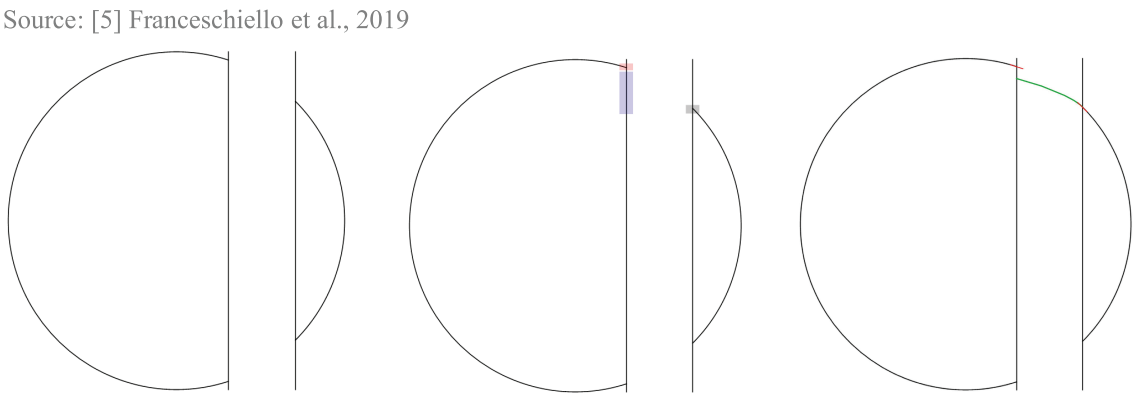

Fig. 4. Round Poggendorff illusion. The parallel lines that obscure parts of a circle break the circle off so that its pieces do not appear to fit together. Fixing the intersection point of a circle and the right parallel line as a departing point for illusory contour, the end point is located somewhere on the indicated segment of the left line. A data adaptive SR minimizer among the family of SR minimizers with terminal set models the illusory contour.

5. Conclusion

In this paper, we have summarized results of a sequence of works related to usage of sub-Riemannian (SR) geometry in image processing and modeling of the human visual system. We extend the model [7] to include data adaptivity via a suitable external cost in the SR metric. We show that data adaptive SR geodesics are useful in real image analysis applications and provide a refined model of V1 that takes into account the presence of a visual stimulus suitable for the explanation of phenomena of geometrical optical illusions.

References

[1] Bekkers, E. J., Duits, R., Mashtakov, A., and Sanguinetti, G. R., A PDE Approach to Data-Driven Sub-Riemannian Geodesics in $SE(2)$, *SIAM J. Imaging Sci.,* 2015, vol. 8, no. 4, pp. 2740–2770.

[2] Duits, R., Ghosh, A., Dela Haije, T., and Mashtakov, A., On Sub-Riemannian Geodesics in $SE(3)$ Whose Spatial Projections do not Have Cusps, *J. Dyn. Control Syst.,* 2016, vol. 22, no. 4, pp. 771–805.

[3] Mashtakov, A. P. and Popov, A. Yu., Extremal Controls in the Sub-Riemannian Problem on the Group of Motions of Euclidean Space, *Regul. Chaotic Dyn.,* 2017, vol. 22, no. 8, pp. 952–957.

[4] Mashtakov, A., Duits, R., Sachkov, Yu., Bekkers, E., and Beschastnyi, I., Tracking of Lines in Spherical Images via Sub-Riemannian Geodesics on $SO(3)$, *J. Math. Imaging Vis.,* 2017, vol. 58, no. 2, pp. 239–264.

[5] Franceschiello, B., Mashtakov, A., Citti, G., and Sarti, A., Geometrical Optical Illusion via Sub-Riemannian Geodesics in the Roto-Translation Group, *Differential Geom. Appl.,* 2019, vol. 65, pp. 55–77.

[6] Petitot, J., The Neurogeometry of Pinwheels As a Sub-Riemannian Contact Structure, *J. Physiol. Paris,* 2003, vol. 97, nos. 2–3, pp. 265–309.

[7] Citti, G. and Sarti, A., A Cortical Based Model of Perceptual Completion in the Roto-Translation Space, *J. Math. Imaging Vis.,* 2006, vol. 24, no. 3, pp. 307–326.

[8] Tax, C. M., Duits, R., Vilanova, A., ter Haar Romeny, B. M., Hofman, P., Wagner, L., Leemans, A., and Ossenblok, P., Evaluating Contextual Processing in Diffusion MRI: Application to Optic Radiation Reconstruction for Epilepsy Surgery, *PLoS ONE,* 2014, vol. 9, no. 7, e101524.

[9] Montgomery, R., *A Tour of Subriemannian Geometries, Their Geodesics and Applications,* Math. Surveys Monogr., vol. 91, Providence, R.I.: AMS, 2002.

[10] Agrachev, A. A. and Sachkov, Yu. L., *Control Theory from the Geometric Viewpoint,* Encyclopaedia Math. Sci., vol. 87, Berlin: Springer, 2004.

[11] Sachkov, Yu. L., Control Theory on Lie Groups, *J. Math. Sci. (N. Y.),* 2009, vol. 156, no. 3, pp. 381–439; see also: *Sovrem. Mat. Fundam. Napravl.,* 2007, vol. 27, pp. 5–59.

[12] Agrachev, A., Barilari, D., and Boscain, U., *A Comprehensive Introduction to Sub-Riemannian Geometry from Hamiltonian Viewpoint,* HAL Id: hal-02019181 (2019), in press.

[13] Sethian, J. A., *Level Set Methods and Fast Marching Methods: Evolving Interfaces in Computational Geometry, Fluid Mechanics, Computer Vision, and Materials Science,* 2nd ed., Cambridge Monogr. Appl. Comput. Math., vol. 3, Cambridge: Cambridge Univ. Press, 1999.

[14] Mirebeau, J.-M., Anisotropic Fast-Marching on Cartesian Grids Using Lattice Basis Reduction, *SIAM J. Numer. Anal.,* 2014, vol. 52, no. 4, pp. 1573–1599.

[15] Sanguinetti, G., Duits, R., Bekkers, E., Janssen, M. H. J., Mashtakov, A., and Mirebeau, J. M., Sub-Riemannian Fast Marching in $SE(2)$, in *Progress in Pattern Recognition, Image Analysis, Computer Vision, and Applications,* A. Pardo, J. Kittler (Eds.), Lecture Notes in Comput. Sci., vol. 9423, Cham: Springer, 2015, pp. 366–374.

[16] Duits, R., Meesters, S. P. L., Mirebeau, J.-M., and Portegies, J. M., Optimal Paths for Variants of the 2D and 3D Reeds-Shepp Car with Applications in Image Analysis, *J. Math. Imaging Vis.,* 2018, vol. 60, no. 6, pp. 816–848.

[17] Bekkers, E., Duits, R., Berendschot, T., and Romeny, B. H., A Multi-Orientation Analysis Approach to Retinal Vessel Tracking, *J. Math. Imaging Vis.,* 2014, vol. 49, no. 3, pp. 583–610.

[18] Peyré, G., Péchaud, M., Keriven, R., and Cohen, L. D., Geodesic Methods in Computer Vision and Graphics, *Found. Trends Comput. Graph. Vis.,* 2010, vol. 5. no. 34, pp. 197–397.